



Atmospheric lifetimes and global warming potentials of atmospherically persistent $N(C_xF_{2x+1})$, $x = 2-4$, perfluoroamines

François Bernard, Dimitrios K Papanastasiou, Robert Portmann, Vassileios Papadimitriou, James B Burkholder

► To cite this version:

François Bernard, Dimitrios K Papanastasiou, Robert Portmann, Vassileios Papadimitriou, James B Burkholder. Atmospheric lifetimes and global warming potentials of atmospherically persistent $N(C_xF_{2x+1})$, $x = 2-4$, perfluoroamines. Chemical Physics Letters, 2020, 744, pp.137089. 10.1016/j.cplett.2020.137089 . hal-02889294

HAL Id: hal-02889294

<https://hal.science/hal-02889294>

Submitted on 13 Sep 2021

HAL is a multi-disciplinary open access archive for the deposit and dissemination of scientific research documents, whether they are published or not. The documents may come from teaching and research institutions in France or abroad, or from public or private research centers.

L'archive ouverte pluridisciplinaire **HAL**, est destinée au dépôt et à la diffusion de documents scientifiques de niveau recherche, publiés ou non, émanant des établissements d'enseignement et de recherche français ou étrangers, des laboratoires publics ou privés.



Distributed under a Creative Commons Attribution| 4.0 International License

**Atmospheric lifetimes and global warming potentials of
atmospherically persistent $N(C_xF_{2x+1})_3$, $x = 2-4$, perfluoroamines**

François Bernard,^{1,2,#} Dimitrios K. Papanastasiou,^{1,2} Robert W. Portmann,¹
Vassileios C. Papadimitriou,^{1,2,3,§} and James B. Burkholder^{1,*}

¹ Earth System Research Laboratory, Chemical Sciences Division, National Oceanic and
Atmospheric Administration, Boulder, Colorado, USA.

² Cooperative Institute for Research in Environmental Sciences, University of Colorado,
Boulder, Colorado, USA.

³ Laboratory of Photochemistry and Chemical Kinetics, Department of Chemistry, University of
Crete, Vassilika Vouton, 71003, Heraklion, Crete, Greece

* Corresponding author.

E-mail address: (James.B.Burkholder@noaa.gov) (J.B. Burkholder)

Current address: Laboratoire de Physique et Chimie de l'Environnement et de l'Espace
(LPC2E), Centre National de la Recherche Scientifique (CNRS), Université d'Orléans,
Observatoire des Sciences de l'Univers en région Centre (OSUC), Orléans, France

§ Permanent Address: Laboratory of Photochemistry and Chemical Kinetics, Department of
Chemistry, University of Crete, Vassilika Vouton, 71003, Heraklion, Crete, Greece.

Abstract

Laboratory studies of the gas-phase $O(^1D)$ reaction and UV photolysis for $N(C_xF_{2x+1})_3$, $x=2-4$) and an evaluation of their atmospheric lifetimes and global warming potentials (GWPs) is reported. The $O(^1D) + PFA$ reactive rate coefficient was measured to be ($10^{-12} \text{ cm}^3\text{molecule}^{-1}\text{s}^{-1}$) 1.10 ± 0.10 , 1.36 ± 0.10 , and 1.69 ± 0.11 and the UV photodissociation yield, $\sigma(\lambda) \times \Phi(\lambda)$, at 193 nm was measured to be ($10^{-23} \text{ cm}^2\text{molecule}^{-1}$) 1.37, <1, <15 for $N(C_2F_5)_3$, $N(C_3F_7)_3$, and $N(C_4F_9)_3$, respectively. Including estimated Lyman- α photolysis leads to total global atmospheric lifetimes of >3,000 years. GWPs on the 100-year time-horizon are estimated to be 9900, 8700, and 7800 for $N(C_2F_5)_3$, $N(C_3F_7)_3$, and $N(C_4F_9)_3$, respectively.

Keywords: Perfluoroamine, UV absorption spectrum, $O(^1D)$ kinetics, atmospheric model, atmospheric lifetime

1. Introduction

$N(C_xF_{2x+1})_3$, perfluoroalkylamines (PFAs), are thermally and chemically stable semi-volatile compounds used in the electronics industry and heat transfer applications. Their industrial use may lead to their direct release into the atmosphere. There is currently very limited data for the atmospheric sources, distribution, and abundance of PFAs. Tropospheric measurements of $N(C_4F_9)_3$ have been reported for urban Toronto, Canada with a mixing ratio of ~ 0.18 ppt [1]. The NILU-Norwegian Institute for Air Research reported a 0.55 ppq abundance of $N(C_4F_9)_3$ in air samples at the Zeppelin station, Ny-Ålesund, Svalbard, Norway ($79^\circ N$, $12^\circ E$) [2]. The detection of other PFAs in the atmosphere has not been reported to date. Previous laboratory studies, including work from this laboratory, have shown that PFAs are potent greenhouse gases due to their strong infrared absorption in the atmospheric window region [1,3,4]. PFAs are expected to be atmospherically persistent compounds and, therefore, have exceptionally large global warming potentials (GWPs) and, thus, their environmental and climate impacts need to be evaluated [5].

A comprehensive evaluation of the environmental impact of PFAs necessitates fundamental laboratory studies of their chemical and photochemical properties. To date, there are no laboratory measurements of the atmospheric removal processes for PFAs available in the literature. In general, quantifying the atmospheric loss processes for an atmospherically persistent compound is challenging due to their low reactivity with atmospheric oxidants, e.g. OH, Cl, NO_3 , and O_3 , and their weak absorption in the ultra-violet region of the spectrum. In their work, Hong et al.[1] assumed the global lifetime for $N(C_4F_9)_3$ to be 500 years, based on similar kinetic and photochemical parameters to that of NF_3 [6].

In this study, the UV photodissociation and $O(^1D)$ reaction rate coefficient, the most likely stratospheric loss processes, for $N(C_2F_5)_3$, $N(C_3F_7)_3$, and $N(C_4F_9)_3$ were measured and the OH reaction rate coefficient estimated. The experimental results from this study were used to evaluate their partial and total global atmospheric lifetimes and global warming potential (GWP) using 2-D atmospheric model calculations and the radiative efficiencies determined in a previous study from this laboratory [3].

2. Experimental Details and Methods

In this study, experiments were performed to: (1) evaluate the UV absorption spectrum and 193 nm photodissociation of $N(C_2F_5)_3$, $N(C_3F_7)_3$, and $N(C_4F_9)_3$, (2) measure the room

temperature reactive rate coefficients for the $O(^1D) + N(C_2F_5)_3$, $N(C_3F_7)_3$, and $N(C_4F_9)_3$ reactions, and (3) estimate rate coefficients for the $OH + N(C_2F_5)_3$, $N(C_3F_7)_3$, and $N(C_4F_9)_3$ reactions. The experimental setups and methods used for these measurements and estimates are described separately below.

2.1 UV Absorption Spectrum and Photodissociation

The gas-phase UV absorption spectra of $N(C_2F_5)_3$, $N(C_3F_7)_3$, and $N(C_4F_9)_3$ were measured between 195 and 350 nm using a 0.5 m spectrograph equipped with a CCD detector. Absorption spectra were measured using a 95 cm Pyrex absorption cell with quartz windows and a 30 W D_2 lamp light source. Perfluoroamine spectra were measured under static and gas flow conditions. The PFA samples were added to the absorption cell from either the head space of the liquid sample or from a dilute gas mixture that was prepared off-line. The PFA concentration in the absorption cell was determined from the measured absorption cell pressure and the ideal gas law. An absorption contribution to the measured spectra from minor PFA sample impurities, however, limited the quantitative determination of PFA absorption spectra.

The photodissociation yields of the PFAs, $\sigma(\lambda) \times \Phi(\lambda)$, where $\sigma(\lambda)$ is the PFA absorption cross section at wavelength λ and Φ is the photolysis quantum yield for loss of the PFA at that wavelength, were measured at 294 K using an actinometry method. The photodissociation yield of the PFAs was measured at 193 nm using pulsed laser photolysis (ArF excimer laser) of static PFA/ N_2O / N_2 gas mixtures:



The PFA photolysis loss rate was measured relative to the photolytic loss of N_2O :



In the presence of a large excess of N_2 , the $O(^1D)$ produced in reaction 2 was rapidly quenched to its ground state:



This relative approach to determine the photodissociation of the PFAs has the advantage that UV absorption by sample impurities, which were a major interference in the UV absorption spectrum measurement, do not interfere with this measurement. Therefore, this approach provides an unequivocal measurement of PFA loss due to UV photolysis at 193 nm.

The photolysis beam passed through the quartz windows of the $\sim 500 \text{ cm}^3$ reactor perpendicular to a set of multi-pass White optics, 125 cm path length, coupled to a Fourier transform infrared spectrometer. A retro reflector outside the exit window enabled a return of

the photolysis beam through the reactor. The overlap of the photolysis beam with the volume of the reactor was relatively small, ~2.4% of the total volume. The reactor was filled with the PFA and N₂O and pressurized to ~600 Torr with N₂ bath gas. Infrared spectra were recorded in 200–1500 cm⁻¹ at a spectral resolution of 1 cm⁻¹. The PFA and N₂O concentrations and their change in concentration with photolysis were measured by infrared absorption during photolysis. The initial PFA concentration was between 1.2×10^{15} and 3.8×10^{15} molecule cm⁻³ and the initial N₂O concentration was $\sim 9 \times 10^{16}$ molecule cm⁻³.

The concentration of PFA remaining after n laser pulses is given by:

$$[\text{PFA}]_n = [\text{PFA}]_0 \times (1 - \sigma_{\text{PFA}}(193 \text{ nm}) \times \Phi_{\text{PFA}}(193 \text{ nm}) \times F)^n \quad (4)$$

where $[\text{PFA}]_0$ is the initial PFA concentration, $[\text{PFA}]_n$ is the PFA concentration after n pulses and F is the photolysis laser fluence. The photolysis laser was operated at 20–30 Hz at a fluence of $\sim 20 \text{ mJ cm}^{-2} \text{ pulse}^{-1}$ as measured with a power meter mounted after the reactor. A similar equation can be written for the N₂O loss. The photochemical conversion of PFA per laser pulse was small and equation (4) is approximated by:

$$\ln\left(\frac{[\text{PFA}]_0}{[\text{PFA}]_n}\right) = n_{\text{PFA}} \times \sigma_{\text{PFA}}(193 \text{ nm}) \times \Phi_{\text{PFA}}(193 \text{ nm}) \times F \quad (5)$$

The PFA photolysis yield was calculated using the relationship:

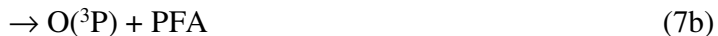
$$\sigma_{\text{PFA}}(193 \text{ nm}) \times \Phi_{\text{PFA}}(193 \text{ nm}) = \sigma_{\text{N}_2\text{O}}(193 \text{ nm}) \times \Phi_{\text{N}_2\text{O}}(193 \text{ nm}) \times \frac{n_{\text{N}_2\text{O}} \ln([\text{PFA}]_0/[\text{PFA}]_n)}{n_{\text{PFA}} \ln([\text{N}_2\text{O}]_0/[\text{N}_2\text{O}]_n)} \quad (6)$$

where the N₂O quantum yield at 193 nm is unity and its absorption cross section at 193 nm is $8.95 \times 10^{-20} \text{ cm}^2 \text{ molecule}^{-1}$ [7].

2.2 O(¹D) Reactive Rate Coefficient

Rate coefficients for the O(¹D) + PFA reaction were measured at room temperature (294 K) using a relative rate technique. The experimental setup and methods have been used previously in this laboratory and only a brief description is given below [8,9].

The relative rate approach used in this work measures the rate coefficient for the reactive channel for the O(¹D) reaction, i.e., PFA loss, reaction 7a:



Rate coefficients were measured with O(¹D) + CHF₃ as the reference reaction:

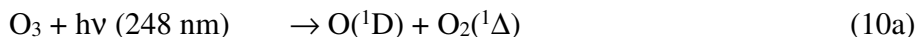


where the recommended total rate coefficient for reaction 8 is $(9.60 \pm 0.48) \times 10^{-12} \text{ cm}^3 \text{ molecule}^{-1} \text{ s}^{-1}$, i.e., for the loss of $\text{O}(^1\text{D})$ [7]. The reactive rate coefficient, k_{8a} , is $2.4 \times 10^{-12} \text{ cm}^3 \text{ molecule}^{-1} \text{ s}^{-1}$ [7]. Assuming that the PFA and CHF_3 are removed solely by reaction with $\text{O}(^1\text{D})$, the PFA and CHF_3 rate coefficients are related by the expression:

$$\ln \left(\frac{[\text{PFA}]_0}{[\text{PFA}]_t} \right) = \frac{k_{\text{PFA}}}{k_{\text{CHF}_3}} \left[\ln \left(\frac{[\text{CHF}_3]_0}{[\text{CHF}_3]_t} \right) \right] \quad (9)$$

where $[\text{PFA}]_0$, $[\text{CHF}_3]_0$, $[\text{PFA}]_t$ and $[\text{CHF}_3]_t$ are the concentrations of the PFA and CHF_3 compound at times t_0 and t , respectively.

The experimental apparatus consisted of a 100 cm long (5 cm i.d.) Pyrex photoreactor. $\text{O}(^1\text{D})$ radicals were produced by 248 nm pulsed laser photolysis (KrF excimer laser, 10 or 50 Hz) of O_3 along the length of the photoreactor:



where the $\text{O}(^1\text{D})$ yield is 0.9 [7]. The initial PFA concentration was in the range $(3.0\text{--}4.1) \times 10^{14} \text{ molecule cm}^{-3}$, while the CHF_3 initial concentration was $\sim 4.5 \times 10^{14} \text{ molecule cm}^{-3}$. The photolysis laser fluence was in the range $1.4\text{--}1.7 \text{ mJ cm}^{-2} \text{ pulse}^{-1}$.

The PFA and CHF_3 loss was monitored by infrared absorption. The photoreactor was coupled to a multi-pass absorption cell (KBr windows, 485 cm path length) of a Fourier transform infrared (FTIR) spectrometer equipped with a liquid nitrogen cooled HgCdTe (MCT) semiconductor detector. The gas mixture was circulated between the photoreactor and the multi-pass absorption cell by a 12 L min^{-1} Teflon diaphragm pump. Infrared spectra were recorded in 100 co-adds between 500 and 4000 cm^{-1} at 1 cm^{-1} resolution.

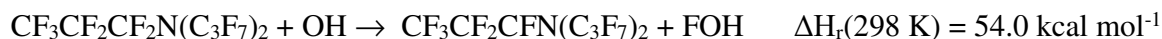
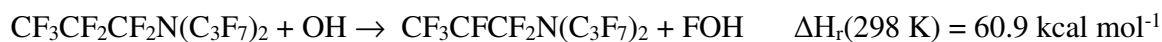
Kinetic measurements were performed by first adding the PFA and CHF_3 to the system and then adding He bath gas to increase the total pressure to $\sim 300 \text{ Torr}$. After the gas mixture was thoroughly mixed, as determined by infrared absorption, a $t = 0$ infrared spectrum was recorded. O_3 , in a He bath gas, was then added slowly to the photoreactor with the photolysis laser and gas circulation on. Infrared spectra were recorded until the change in the PFA and CHF_3 concentration ceased to decrease significantly, primarily due to the buildup of O_2 in the system.

2.3 Computational Methods

The reaction of perfluoroamines with OH radicals is expected to make a negligible contribution to their atmospheric loss. Here, we used theoretical methods to estimate upper-

limits for the reaction rate coefficients, at 298 K, for the reaction of OH radicals with $\text{N}(\text{C}_3\text{F}_7)_3$. The other amines are expected to have a similar reactivity. Optimized structures, normal mode vibrational frequencies, and thermochemical parameters for $\text{N}(\text{C}_3\text{F}_7)_3$, OH, and reaction products were calculated using the Gaussian 09 program suite [10]. The DFT functional B97-1 with the 6-311 ++ G(2df,2p) basis set, with ultrafine grid numerical integration, was used for all calculations.

Reaction channels were explored where either OH abstracts an F atom to form FOH + radical, or where the OH radical adds to the amine to form a hydroxylamine and a C_3F_7 radical (i.e., C-N bond cleavage):



Each of these reactions are endothermic and we have followed the approach adopted by the IUPAC and NASA kinetic data evaluation panels to estimate a rate coefficient assuming a pre-exponential factor, A , $1 \times 10^{-11} \text{ cm}^3 \text{ molecule}^{-1} \text{ s}^{-1}$ in this case, and a lower-limit activation energy equal to that of the reaction endothermicity. The F-atom abstraction channels have extremely low 298 K rate coefficients, $<2.5 \times 10^{-51} \text{ cm}^3 \text{ molecule}^{-1} \text{ s}^{-1}$. The hydroxylamine formation channel is calculated to have a rate coefficient of $<2.2 \times 10^{-19} \text{ cm}^3 \text{ molecule}^{-1} \text{ s}^{-1}$. Channel 11d is, however, expected to have a significant activation barrier to reaction, which was not evaluated in this work, due to steric hinderance towards product formation. The barrier would make the reaction rate coefficient considerably less.

2.4 Materials

$\text{N}(\text{C}_2\text{F}_5)_3$ (perfluorotriethylamine, CAS# 359-70-6, 97%), $\text{N}(\text{C}_3\text{F}_7)_3$ (perfluorotripropylamine, CAS# 338-83-0, ~94.5%), and $\text{N}(\text{C}_4\text{F}_9)_3$ (perfluorotributylamine, CAS# 311-89-7, 99.5%) were obtained commercially with the stated purity given in parenthesis. The perfluoroamines are liquids at room temperature and were degassed in several freeze (77 K)-pump-thaw cycles and stored under vacuum in Pyrex reservoirs. He (UHP, 99.999%), N_2 (UHP, 99.999%), and N_2O (>99.99%) were used as supplied. Ozone was produced by flowing O_2 through a silent discharge and collected on silica gel in a trap at 195 K. Ozone was introduced into the $\text{O}(^1\text{D})$ reaction cell by passing a small flow of He through the trap.

For the O(¹D) reaction and photodissociation studies, PFA were introduced in the reactors using dilute PFA gas mixtures prepared manometrically in He and N₂ bath gas. Mixtures were prepared in 12 L Pyrex bulbs with the following mixing ratios: 0.01447% in He for (C₂F₅)₃N, 0.0167% in He and 0.01925% in N₂ for (C₃F₇)₃N and 0.01233% in He and 0.01403% in N₂ for (C₄F₉)₃N). Pressures were measured using calibrated capacitance manometers. Uncertainties given throughout the paper are 2σ unless noted otherwise.

3. Results and Discussion

3.1 UV absorption spectrum and photodissociation

UV absorption spectra of the PFA samples (taken from the liquid sample head space) were measured over the 200–350 nm wavelength range. Absorption was observed between 200 and 300 nm for N(C₂F₅)₃ and between 200 and 250 nm for N(C₃F₇)₃ and N(C₄F₉)₃. The measured absorption spectra were, however, irreproducible, due to changing impurity contributions, while the effective cross sections were small, with values of less than 10⁻²⁰ cm² molecule⁻¹ at 200 nm. The weak PFA UV absorption makes the measurements highly susceptible to interference by minor sample impurities that absorb strongly in the UV. Vacuum distillation of the liquid PFA samples did not yield consistent UV spectra. Examples of the measured spectra are given in the Supporting Information (**Figure S1**). However, in all cases, it was clear that absorption at wavelengths greater than 290 nm was not detectable, i.e., the corresponding effective PFA absorption cross section was <10⁻²² cm² molecule⁻¹ in this wavelength region. Although we were unable to measure quantitative PFA UV absorption spectra, the measurements demonstrate weak absorption in the short (195–210 nm) and long (>290 nm) wavelength actinic regions.

A summary of the experimental conditions and the PFA photolysis yield results are given in **Table 1**. PFA photodissociation at 193 nm was found to be inefficient and, thus, required fairly long exposure to the photolysis laser to achieve measurable PFA losses. A representative set of photolysis data is shown in **Figure 1**. Experiments were performed with a total number of photolysis pulses in the range (3.6–4.5) × 10⁵, corresponding to ~5 hours total photolysis time. The photochemical conversion rate of N₂O exceeded that of the PFA by at least two orders of magnitude.

Table 1. Experimental conditions and results for the 193 nm photodissociation of $\text{N}(\text{C}_2\text{F}_5)_3$, $\text{N}(\text{C}_3\text{F}_7)_3$, and $\text{N}(\text{C}_4\text{F}_9)_3$ at 294 K

| Perfluoroamine (PFA) | [PFA] (10^{15} molecule cm^{-3}) | $[\text{N}_2\text{O}]$ (10^{15} molecule cm^{-3}) | $\sigma(\lambda) \times \Phi(\lambda)$ ($\text{cm}^2 \text{ molecule}^{-1}$) |
|------------------------------------|--|---|---|
| $\text{N}(\text{C}_2\text{F}_5)_3$ | 1.2 | 9.2 | 1.37×10^{-23} |
| $\text{N}(\text{C}_3\text{F}_7)_3$ | 3.8 | 9.1 | $<1 \times 10^{-23}$ |
| $\text{N}(\text{C}_4\text{F}_9)_3$ | 2.5 | 8.9 | $<1.5 \times 10^{-22}$ |

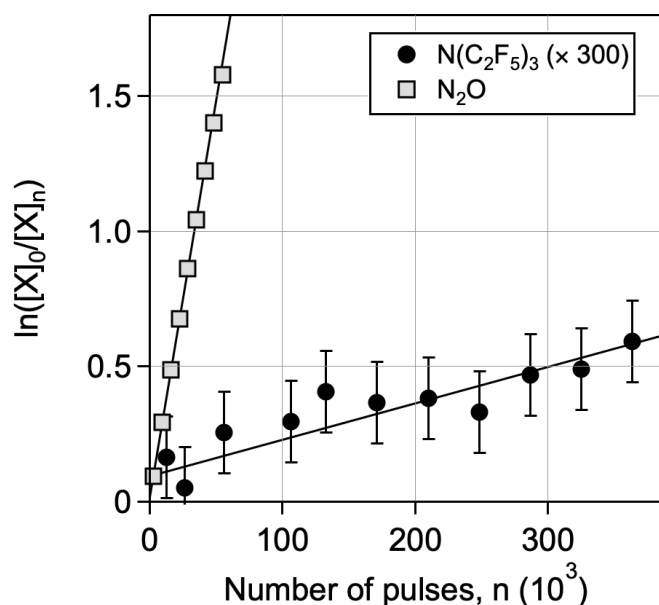


Figure 1. Loss of $\text{N}(\text{C}_2\text{F}_5)_3$ (circles) and N_2O (squares) following 193 nm pulsed laser photolysis. The $\text{N}(\text{C}_2\text{F}_5)_3$ data has been multiplied by 300 for improved clarity. The lines are linear least-squares fits to the data. The error bars on the $\text{N}(\text{C}_2\text{F}_5)_3$ data points represent the precision of the infrared spectral analysis. The precision error bars for N_2O are smaller than the symbol size.

The background loss of PFA from the experimental apparatus measured in the absence of photolysis was an additional issue in the interpretation of the photolysis results. Background loss was measured before and after the photolysis experiments and the average value subtracted from the observed PFA loss rate. For $\text{N}(\text{C}_2\text{F}_5)_3$, the background loss was negligible, but significant for $\text{N}(\text{C}_3\text{F}_7)_3$ and $\text{N}(\text{C}_4\text{F}_9)_3$ over the long duration of the experiment. The first-order rate coefficient for the dark loss of $\text{N}(\text{C}_3\text{F}_7)_3$ were 2.02×10^{-7} and $1.82 \times 10^{-7} \text{ s}^{-1}$, before and after respectively. The total decay rate of $\text{N}(\text{C}_3\text{F}_7)_3$ during 193 nm photolysis was $2.92 \times 10^{-7} \text{ s}^{-1}$. For $\text{N}(\text{C}_4\text{F}_9)_3$,

dark loss rate coefficients were 1.40×10^{-6} and $4.56 \times 10^{-7} \text{ s}^{-1}$. The total decay rate of $\text{N}(\text{C}_4\text{F}_9)_3$ during photolysis was $1.41 \times 10^{-6} \text{ s}^{-1}$. $\sigma(193 \text{ nm}, 294 \text{ K}) \times \phi(193 \text{ nm}, 294 \text{ K})$ were determined to be 1.37×10^{-23} , $<1 \times 10^{-23}$ and $<1.5 \times 10^{-22} \text{ cm}^2 \text{ molecule}^{-1}$ for $\text{N}(\text{C}_2\text{F}_5)_3$, $\text{N}(\text{C}_3\text{F}_7)_3$, and $\text{N}(\text{C}_4\text{F}_9)_3$, respectively.

Although photolysis yields were only measured at 193 nm, the UV absorption spectrum measurements implies that photolysis yields at longer wavelengths would be lower for wavelength greater than 193 nm.

3.2 O(¹D) Reactive Rate Coefficient

Table 2 provides a summary of the 294 K O(¹D) + PFA relative rate results obtained in this work. **Figure 2** shows the raw relative rate data for the $\text{N}(\text{C}_2\text{F}_5)_3$, $\text{N}(\text{C}_3\text{F}_7)_3$, and $\text{N}(\text{C}_4\text{F}_9)_3$ reactions that includes multiple independent measurements for the $\text{N}(\text{C}_3\text{F}_7)_3$ reaction. The measured O(¹D) rate coefficients show a slight systematic increase in reactivity with increased carbon chain length in the PFA. Due to the low reactivity of the PFAs, the total loss of PFA achieved with this experimental approach was <15%. It is worth noting that PFA loss in the absence of O(¹D) production was found to be negligible. The low conversion leads to greater measurement precision uncertainty when compared with typical OH and Cl-atom relative rate measurements that typically have precisions of a few percent. The fit precision uncertainties given in **Table 2** are ~5%, or less. The independent experimental $\text{N}(\text{C}_3\text{F}_7)_3$ reaction measurement results agree to within ~15%. The final rate coefficient for the $\text{N}(\text{C}_3\text{F}_7)_3$ reaction was obtained from the least-square analysis of all the data.

Table 2. Summary of experimental conditions and rate coefficients, $k(294 \text{ K})$, obtained in this work for the O(¹D) + $\text{N}(\text{C}_2\text{F}_5)_3$, $\text{N}(\text{C}_3\text{F}_7)_3$, and $\text{N}(\text{C}_4\text{F}_9)_3$ reactions using a relative rate technique

| Perfluoroamine (PFAm) | [PFA] ($10^{14} \text{ molecule cm}^{-3}$) | [CHF ₃] ($10^{14} \text{ molecule cm}^{-3}$) | k/k_{Ref}^a | k ($10^{-12} \text{ cm}^3 \text{ molecule}^{-1} \text{ s}^{-1}$) ^a |
|------------------------------------|---|---|----------------------|--|
| $\text{N}(\text{C}_2\text{F}_5)_3$ | 3.6 | 4.6 | 0.455 ± 0.019 | 1.10 ± 0.10 |
| $\text{N}(\text{C}_3\text{F}_7)_3$ | 4.0 | 4.4 | 0.587 ± 0.011 | 1.41 ± 0.10 |
| | 3.9 | 4.4 | 0.649 ± 0.018 | 1.56 ± 0.12 |
| | 4.1 | 4.4 | 0.545 ± 0.009 | 1.31 ± 0.09 |
| | | | 0.563 ± 0.012^b | 1.36 ± 0.10 |
| $\text{N}(\text{C}_4\text{F}_9)_3$ | 3.0 | 4.4 | 0.703 ± 0.011 | 1.69 ± 0.11 |

^a 2σ fit precision uncertainty

^b Rate coefficient ratio was obtained from a fit of all N(C₃F₇)₃ data combined

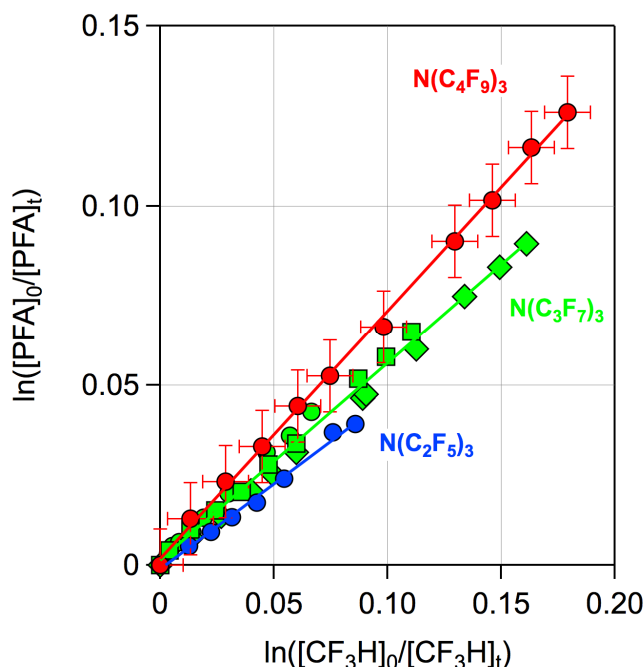


Figure 2. Relative rate data for the O(¹D) + N(C₂F₅)₃, N(C₃F₇)₃, and N(C₄F₉)₃ reactions with CHF₃ used as the reference compound. The different symbols for the N(C₃F₇)₃ reaction represent independent experiments. The lines are weighted linear least-squares fits to the data (a fit to the combined data for N(C₃F₇)₃). For clarity, the estimated measurement uncertainty is only shown for the N(C₄F₉)₃ reaction. The obtained rate coefficient ratios and derived O(¹D) rate coefficient results are given in **Table 2**.

The measured rate coefficient ratios were placed on an absolute basis using the O(¹D) rate coefficient of CHF₃ (channel 8a), $(2.4 \pm 0.12) \times 10^{-12} \text{ cm}^3 \text{ molecule}^{-1} \text{ s}^{-1}$ [7]. Overall, the O(¹D) reactive rate coefficients are slow, but consistent with values reported for other highly fluorinated compounds [7]. The estimated absolute uncertainty in the O(¹D) reactive rate coefficients was determined from the precision and reproducibility of the experimental data and the uncertainty in the CHF₃ reference compound rate coefficient and estimated to be 9% for N(C₂F₅)₃ and 7% for N(C₃F₇)₃ and N(C₄F₉)₃.

4. Atmospheric Lifetimes and Global Warming Potentials

The NOCAR 2-D model was used to estimate the PFA globally averaged partial and total atmospheric lifetimes. The 2-D model details can be found elsewhere [11]. The total globally averaged atmospheric lifetime was computed as a combination of the partial global lifetimes:

$$\frac{1}{\tau_{\text{Total}}} = \frac{1}{\tau_{\text{OH}}} + \frac{1}{\tau_{\text{O}(^1\text{D})}} + \frac{1}{\tau_{\text{UV}}} + \frac{1}{\tau_{\text{Lyman-}\alpha}}$$

Loss of the perfluoroamines due to reaction with the OH radical was shown earlier to most likely be negligible and, therefore, is not considered further. The O(¹D) + PFA reaction represents an atmospheric loss processes that occurs primarily in the stratosphere. The 2-D model calculated atmospheric lifetime with respect to O(¹D) reaction, using the reactive rate coefficients measured in this work, was estimated to be >20,000 years for each of the PFAs included in this study.

PFA photolysis was determined in this study at 193 nm. The majority of stratospheric UV photolysis however is expected to occur in the wavelength region between 195 and 220 nm. For an accurate determination of photolysis lifetimes, the absorption cross sections in this wavelength region is needed. Our measured photolysis yield at 193 nm was used along with an assumed decrease of a factor of 10 every 10 nm toward longer wavelengths for the UV photolysis lifetime calculations. For comparison, the NF₃ UV absorption spectrum decreases at about this rate for wavelengths greater than 200 nm [6]. UV photolysis in the 200–220 nm wavelength region is, an inefficient atmospheric loss process leading to a calculated global atmospheric lifetime of greater than 50,000 years. Note that model calculations of atmospheric lifetimes this long have a high degree of uncertainty and should not be considered quantitative.

There are no PFA absorption cross section data at Lyman-α (121.567 nm) currently available in the literature. On the basis of a comparison with other fluorinated compounds, PFAs are expected to absorb strongly in the VUV with a Lyman-α cross section of ~10⁻¹⁷ cm² molecule⁻¹. The partial global lifetime for Lyman-α photolysis was estimated to be >4,500 years. A smaller Lyman-α absorption cross section would yield a longer lifetime. Although Lyman-α photolysis represents a long atmospheric lifetime, it may represent a significant atmospheric loss process for PFAs. A combination of the estimated lifetimes leads to PFA atmospheric lifetimes of at least ~3,000 years as summarized in Table 3.

Table 3. Partial and total global atmospheric lifetime, radiative efficiency (RE), and global warming potential (GWP) for N(C₂F₅)₃, N(C₃F₇)₃, and N(C₄F₉)₃^a

| Perfluoroamine (PFAM) | τ_{UV}^b (Years) | $\tau_{O(^1D)}$ (Years) | $\tau_{Lyman-\alpha}^c$ (Years) | τ_{Total} (Years) | RE ^d (W m ⁻² ppb ⁻¹) | GWP ₁₀₀ ^e |
|--|--------------------------|----------------------------|------------------------------------|---------------------------|---|---------------------------------|
| N(C ₂ F ₅) ₃ | $> 5 \times 10^5$ | 3×10^4 | 4500 | 3880 | 0.61 | 9900 |
| N(C ₃ F ₇) ₃ | $> 8 \times 10^5$ | 2.5×10^4 | 4500 | 3795 | 0.75 | 8700 |
| N(C ₄ F ₉) ₃ | $> 5 \times 10^4$ | 2.0×10^4 | 4500 | 3650 | 0.87 | 7800 |

^a Lifetimes were estimated based on 2-D atmospheric model calculations (see text); ^b Assuming $\sigma(\lambda)$ decreases of a factor of 10 every 10 nm for wavelengths greater than 193 nm; ^c Lifetime estimated assuming $\sigma(\text{Lyman-}\alpha) = 1 \times 10^{-17} \text{ cm}^2 \text{ molecule}^{-1}$; ^d RE values taken from Bernard et al. [3]; ^e Rounded-off estimated GWP relative to CO₂ for the 100-year time horizon

In a recent study from this laboratory, the radiative efficiencies (REs) for perfluorotriethylamine (N(C₂F₅)₃), perfluorotripropylamine (N(C₃F₇)₃), and perfluorotributylamine (N(C₄F₉)₃) were determined [3]. Combining these values with the atmospheric lifetimes obtained in the present work leads to large global warming potentials on the 100-yr time horizon for the PFAs as given in Table 3. The GWP values of the PFAs included in this study are of comparable magnitude to those of other highly fluorinated persistent atmospheric traces gases such as NF₃, SF₆, and CF₄, which have GWP₁₀₀ values of 15750, 23500, and 6630, respectively [5].

7. Conclusions

In this study, laboratory experiments were conducted that define the global annually averaged partial and total atmospheric lifetimes of N(C₂F₅)₃, N(C₃F₇)₃, and N(C₄F₉)₃. The O(¹D) reaction and UV photolysis loss processes evaluated in this work were used in 2-D atmospheric model simulations to evaluate the global total atmospheric lifetimes. PFAs are primarily removed in the stratosphere and lower mesosphere such that their removal and lifetimes depend on the modeled transport and turnover times for these regions of the atmosphere. Although the lifetimes are clearly long and GWPs large, a multi-model analysis would be useful to better define the possible range in lifetimes and GWPs for the atmospherically persistent PFAs included in this study.”

It was shown that PFAs are atmospherically persistent potent greenhouse gases (GHGs) with GWPs on the 100-year time horizon in the range 7800-9900 for N(C₂F₅)₃, N(C₃F₇)₃, and N(C₄F₉)₃. GWPs were calculated using the radiative efficiencies reported by Bernard et al. [3]

348 and atmospheric lifetimes from this work, see Table 3. The present results provide a
349 fundamental basis for guiding future policy decisions regarding the potential release of
350 perfluoroamines into the environment.

351 **Acknowledgments**

352 This work was supported in part by NOAA's Climate Program Office Atmospheric
353 Chemistry, Carbon Cycle, and Climate Program and NASA's Atmospheric Composition
354 Program.

355 **Author Contributions:**

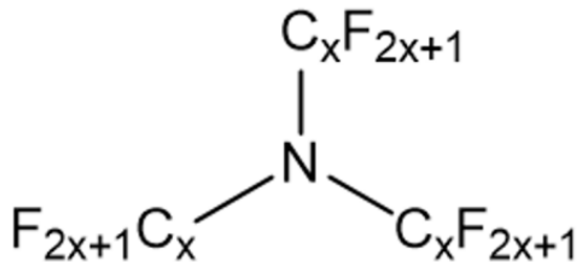
356 FB, DP, VP, and JB, experimental measurements and data analysis; DP and VP,
357 theoretical calculations; RP, atmospheric modeling; FB and JB, manuscript writing
358

References

- [1] A.C. Hong, C.J. Young, M.D. Hurley, T.J. Wallington, S.A. Mabury, Perfluorotributylamine: A novel long-lived greenhouse gas, *Geophys. Res. Lett.* 40 (2013) 6010-6015.
- [2] Norwegian Institute for Air Research, "Screening Programme 2017 – AMAP Assessment compounds", NILU report 21/2018, 2018.
- [3] F. Bernard, D.K. Papanastasiou, V.C. Papadimitriou, J.B. Burkholder, Infrared absorption spectra of $N(C_xF_{2x+1})_3$, $x = 2-5$ perfluoroamines, *J. Quant. Spectrosc. & Rad. Transfer* 211 (2018) 166-171.
- [4] P.J. Godin, A. Cabaj, S. Conway, A.C. Hong, K. Le Bris, S.A. Mabury, K. Strong, Temperature-dependent absorption cross-sections of perfluorotributylamine, *J. Mol. Spectrosc.* 323 (2016) 53-58.
- [5] WMO, (World Meteorological Organization), Scientific Assessment of Ozone Depletion: 2018, Global Ozone Research and Monitoring Project–Report No. 58, 588 pp., Geneva, Switzerland, 2018.
- [6] V.C. Papadimitriou, M.R. McGillen, E.L. Fleming, C.H. Jackman, J.B. Burkholder, NF_3 : UV absorption spectrum temperature dependence and the atmospheric and climate forcing implications, *Geophys. Res. Lett.* 40 (2013) 440-445.
- [7] J.B. Burkholder, S.P. Sander, J. Abbatt, J.R. Barker, R.E. Huie, C.E. Kolb, M.J. Kurylo, V.L. Orkin, D.M. Wilmouth, P.H. Wine, "Chemical Kinetics and Photochemical Data for Use in Atmospheric Studies, Evaluation No. 18," JPL Publication 15-10, Jet Propulsion Laboratory, Pasadena, 2015
<http://jpldataeval.jpl.nasa.gov>, (2015)
- [8] M. Baasandorj, E.L. Fleming, C.H. Jackman, J.B. Burkholder, $O(^1D)$ kinetic study of key ozone depleting substances and greenhouse gases, *J. Phys. Chem. A* 117 (2013) 2434-2445.
- [9] M. Baasandorj, B.D. Hall, J.B. Burkholder, Rate coefficients for the reaction of $O(^1D)$ with the atmospherically long-lived greenhouse gases NF_3 , SF_3CF_3 , CHF_3 , C_2F_6 , $c-C_3F_8$, $n-C_5F_{12}$, and $n-C_6F_{14}$, *Atmos. Chem. Phys.* 12 (2012) 11753-11764.
- [10] M.J. Frisch, G.W. Trucks, H.B. Schlegel, G.E. Scuseria, M.A. Robb, J.R. Cheeseman, G. Scalmani, V. Barone, G.A. Petersson, H. Nakatsuji, X. Li, M. Caricato, A. Marenich, J. Bloino, B.G. Janesko, R. Gomperts, B. Mennucci, H.P. Hratchian, J.V. Ortiz, A.F. Izmaylov, J.L. Sonnenberg, D. Williams-Young, F. Ding, F. Lipparini, F. Egidi, J. Goings, B. Peng, A. Petrone, T. Henderson, D. Ranasinghe, V.G. Zakrzewski, J. Gao, N. Rega, G. Zheng, W. Liang, M. Hada, M. Ehara, K. Toyota, R. Fukuda, J. Hasegawa, M. Ishida, T. Nakajima, Y. Honda, O. Kitao, H. Nakai, T. Vreven, K. Throssell, J. J. A. Montgomery, J.E. Peralta, F. Ogliaro, M. Bearpark, J.J. Heyd, E. Brothers, K.N. Kudin, V.N. Staroverov, T. Keith, R. Kobayashi, J. Normand, K. Raghavachari, A. Rendell, J.C. Burant, S.S. Iyengar, J. Tomasi, M. Cossi, J.M. Millam, M. Klene, C. Adamo, R. Cammi, J.W. Ochterski, R.L. Martin, K. Morokuma, O. Farkas, J.B. Foresman, D.J. Fox, Gaussian 09, Revision A.02, Gaussian, Inc., Wallingford CT (2016)
- [11] R.W. Portmann, S. Solomon, Indirect Radiative Forcing of the Ozone Layer During the 21st Century. , *Geophys. Res. Lett.* 34 (2007) L02813.

GAS-PHASE LOSS PROCESSES

Perfluoroamines (PFAs)



$x = 2 - 4$

Mesosphere:

- Lyman- α photolysis

Stratosphere:

- UV photolysis
- $\text{O}(^1\text{D})$ reaction

Troposphere:

- OH reaction

**Atmospheric
lifetime (τ)**

**Radiative
efficiencies
(RE)**

**Global Warming
Potential (GWP)**

$$\text{GWP} = \frac{RE \times \tau \times \left[1 - e^{-\tau/\tau} \right]}{\text{Int RF}_{\text{CO}_2}(T)}$$

T: 100-year time horizon